Supporting Information

The influence of peptide context on signalling and trafficking of glucagon-like peptide-1 receptor biased agonists

Zijian Fang[1,2,#], Shiqian Chen[1,#], Philip Pickford[1], Johannes Broichhagen[3], David J Hodson[4,5], Ivan R Corrêa Jr[6], Sunil Kumar[7], Frederik Görlitz[7], Chris Dunsby[7], Paul MW French[7], Guy A Rutter[8], Tricia Tan[1], Stephen R Bloom[1], Alejandra Tomas[8,*], and Ben Jones[1,*].

1. Section of Endocrinology and Investigative Medicine, Imperial College London, London, United Kingdom.

2. Present address: Wellcome Trust – Medical Research Council Cambridge Stem Cell Institute and Department of Haematology, University of Cambridge, Cambridge CB2 0AW

3. Leibniz-Forschungsinstitut für Molekulare Pharmakologie (FMP), Department Chemical Biology, Robert-Rössle-Strasse 10, 13125 Berlin, Germany.

4. Institute of Metabolism and Systems Research (IMSR), and Centre of Membrane Proteins and Receptors (COMPARE), University of Birmingham, Birmingham, United Kingdom.

5. Centre for Endocrinology, Diabetes and Metabolism, Birmingham Health Partners, Birmingham, United Kingdom.

6. New England Biolabs, Ipswich, USA.

7. Department of Physics, Imperial College London, London, United Kingdom.

8. Section of Cell Biology and Functional Genomics, Imperial College London, London, United Kingdom.

* Corresponding authors: Ben Jones (ben.jones@imperial.ac.uk) and Alejandra Tomas (a.tomas-catala@imperial.ac.uk)

# These authors contributed equally.

Table of contents

Table S-1.

Ligand	$T_{1/2}$ (HEK293)	$T_{1/2}$ (INS-1 832/3)	Ratio
GLP-1	9.9	4.8	2.1
GLP-1-phe1	16.9	10.3	1.6
Chi1	10.4	5.6	1.9
Chi1-phe1	n.c.	16.8	n.c.
Chi2	10.0	5.6	1.8
Chi2-phe1	17.2	9.0	1.9
Chi3	10.2	5.0	2.0
Chi3-phe1	17.4	13.4	1.3
Ex-ala2	8.9	4.6	1.9
Ex-ala2-phe1	16.4	10.1	1.6
Ex4	8.9	4.6	1.9
Ex4-phe1	n.c.	n.c.	n.c.
GLP-1-gly2	10.9	5.0	2.2
GLP-1-gly2-phe1	n.c.	n.c.	n.c.

Table S-1: SNAP-GLP-1R internalisation rates for each ligand in HEK293 and INS-1 832/3 cells. Internalisation half-times were calculated by fitting a 4-parameter logistic curve to pooled DERET data expressed as fold-increase from baseline, with "basal response" constrained to a fixed value of 1. Ratio indicates the ratio of internalisation $t_{1/2}$ for HEK293 *versus* INS-1 832/3. "n.c." indicates not calculable.

Figure S-1

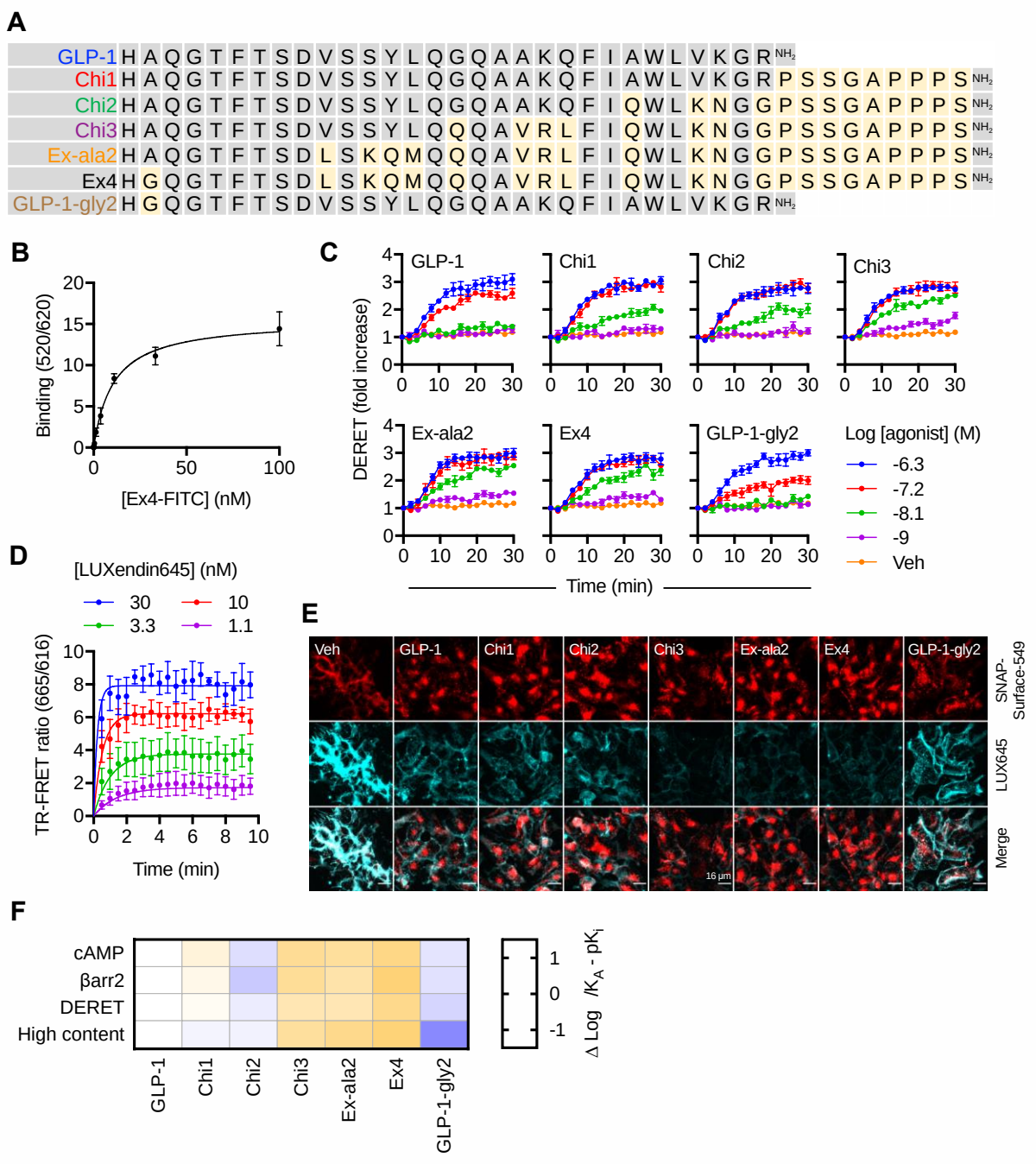

Figure S-1. Additional binding, signalling, and trafficking data for chimeric GLP-1R ligands. (**A**) Peptide agonist sequences in single letter amino acid code, with exendin-4-specific residues highlighted in gold. (**B**) Saturation binding of exendin-4-FITC in HEK293-SNAP-GLP-1R cells, *n*=5, see also Figure 1B. (**C**) Kinetic traces for GLP-1R internalisation in HEK293-SNAP-GLP-1R cells stimulated with indicated concentration of agonist, measured by DERET, *n*=4, relates to Figure 1E. (**D**) TR-FRET measurements of LUXendin645 binding to

Lumi4-Tb-labelled SNAP-GLP-1R in HEK293 cells, *n*=3, kinetic binding curve fitting of pooled data shown. (**E**) Widefield microscopy images of HEK293-SNAP-GLP-1R cells labelled with SNAP-Surface-549 prior to stimulation with 1 µM agonist for 30 minutes, followed by 60 minute recycling and labelling of surface GLP-1Rs with LUXendin645 (100 nM); representative images of *n*=5 independent experiments shown, with identical brightness and contrast settings across all single-channel images; scale bar = 16 µm. (**F**) Heatmap representation of coupling between occupancy and cAMP, β-arrestin-2 recruitment and endocytosis (measured by DERET and high content microscopy) signalling, determined by subtraction of pK_i from log $\boldsymbol{\tau}/K_A$ values for each pathway (see Tables 2 and 3) and subsequently normalised to GLP-1. Data represented as mean ± SEM.

Figure S-2

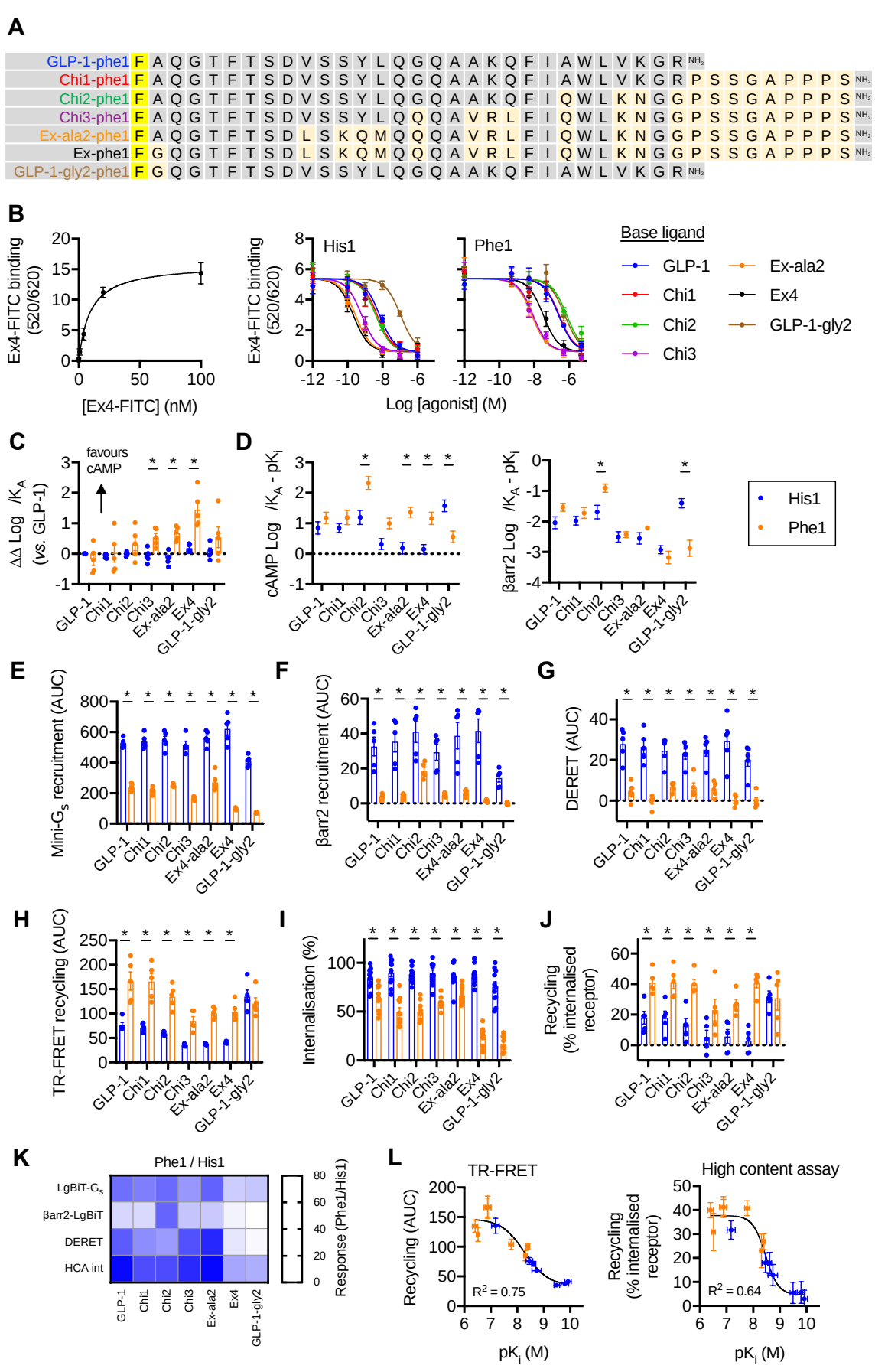
A
GLP-1-phe1 F A Q G T F T S D V S S Y L Q G Q A A K Q F I A W L V K G R NH2
Chi1-phe1 F A Q G T F T S D V S S Y L Q G Q A A K Q F I A W L V K G R P S S G A P P P S NH2
Chi2-phe1 F A Q G T F T S D V S S Y L Q G Q A A K Q F I Q W L K N G G P S S G A P P P S NH2
Chi3-phe1 F A Q G T F T S D V S S Y L Q G Q A V R L F I Q W L K N G G P S S G A P P P S NH2
Ex-ala2-phe1 F A Q G T F T S D L S K Q M Q Q Q A V R L F I Q W L K N G G P S S G A P P P S NH2
Ex-phe1 F G Q G T F T S D L S K Q M Q Q Q A V R L F I Q W L K N G G P S S G A P P P S NH2
GLP-1-gly2-phe1 F G Q G T F T S D V S S Y L Q G Q A A K Q F I A W L V K G R NH2
B
Ex4-FITC binding (520/620)
[Ex4-FITC] (nM)
His1
Phe1
Log [agonist] (M)
Base ligand
GLP-1
Chi1
Chi2
Chi3
Ex-ala2
Ex4
GLP-1-gly2
C
ΔΔ Log /KA (vs. GLP-1)
favours cAMP
D
cAMP Log /KA - pKi
βarr2 Log /KA - pKi
His1
Phe1
E
Mini-Gs recruitment (AUC)
F
βarr2 recruitment (AUC)
G
DERET (AUC)
H
TR-FRET recycling (AUC)
I
Internalisation (%)
J
Recycling (% internalised receptor)
K
Phe1 / His1
LgBiT-Gs
βarr2-LgBiT
DERET
HCA int
Response (Phe1/His1)
L
TR-FRET
Recycling (AUC)
R2 = 0.75
pKi (M)
High content assay
Recycling (% internalised receptor)
R2 = 0.64
pKi (M)

Figure S-2. Phe1-substituted ligand evaluation. (**A**) Phe1 peptide sequences in single letter amino acid code, with exendin-4-specific residues highlighted in gold. (**B**) Equilibrium binding studies in HEK293-SNAP-GLP-1R cells, showing saturation binding of exendin-4-FITC measured by TR-FRET, with parallel measurements of 4 nM exendin-4-FITC binding in competition with indicated concentration of unlabelled agonist, *n*=5. (**C**) Alternative depiction of data shown by heatmap in Figure 2A, indicating bias ($\Delta\Delta$ log $\boldsymbol{\tau}/K_A$) of each ligand relative to GLP-1. (**D**) Representation of coupling between occupancy and cAMP and β-arrestin-2 responses in PathHunter CHO-K1-βarr2-EA-GLP-1R cells, determined by subtraction of pK_i from log $\boldsymbol{\tau}/K_A$ values for each pathway (see Table 3), with error propagation, with each ligand pair compared by one-way ANOVA with Sidak's test. (**E**) AUC analysis for LgBiT-mini-G_s recruitment (Figure 2B), with statistical comparison by one-way randomised block ANOVA with Sidak's test to compare bias for each His1 / Phe1 ligand pair. (**F**) As for (E) but for βarr2-LgBiT recruitment (Figure 2C). (**G**) As for (E) but for internalisation measured by DERET (Figure 2D). (**H**) As for (E) but for GLP-1R recycling measured by TR-FRET (Figure 2E). (**I**) Quantification of GLP-1R internalisation in HEK293-SNAP-GLP-1R cells after 1 μM ligand treatment for 30 minutes, measured by high content microscopy analysis, *n*=11, with statistical comparison by one-way randomised block ANOVA with Sidak's test to compare bias for each His1 / Phe1 ligand pair. (**J**) As for I, but for GLP-1R recycling after 1 μM ligand pre-treatment, *n*=5. (**K**) Alternative representation of data shown in Figures 2B, 2C, 2D and Figure S-2I, with Phe1 ligand responses expressed relative to the equivalent His1 ligand. (**L**) Relationship between agonist binding affinity (see Table 4) and GLP-1R recycling measuremed by TR-FRET (see Figure 2E) and high content microscopy (see Figure S-2J), with 4-parameter logistic fits and goodness-of-fit shown. *p<0.05 by statistical test indicated in the text. Data represented as mean ± SEM, with individual replicates shown in some cases.

Figure S-3

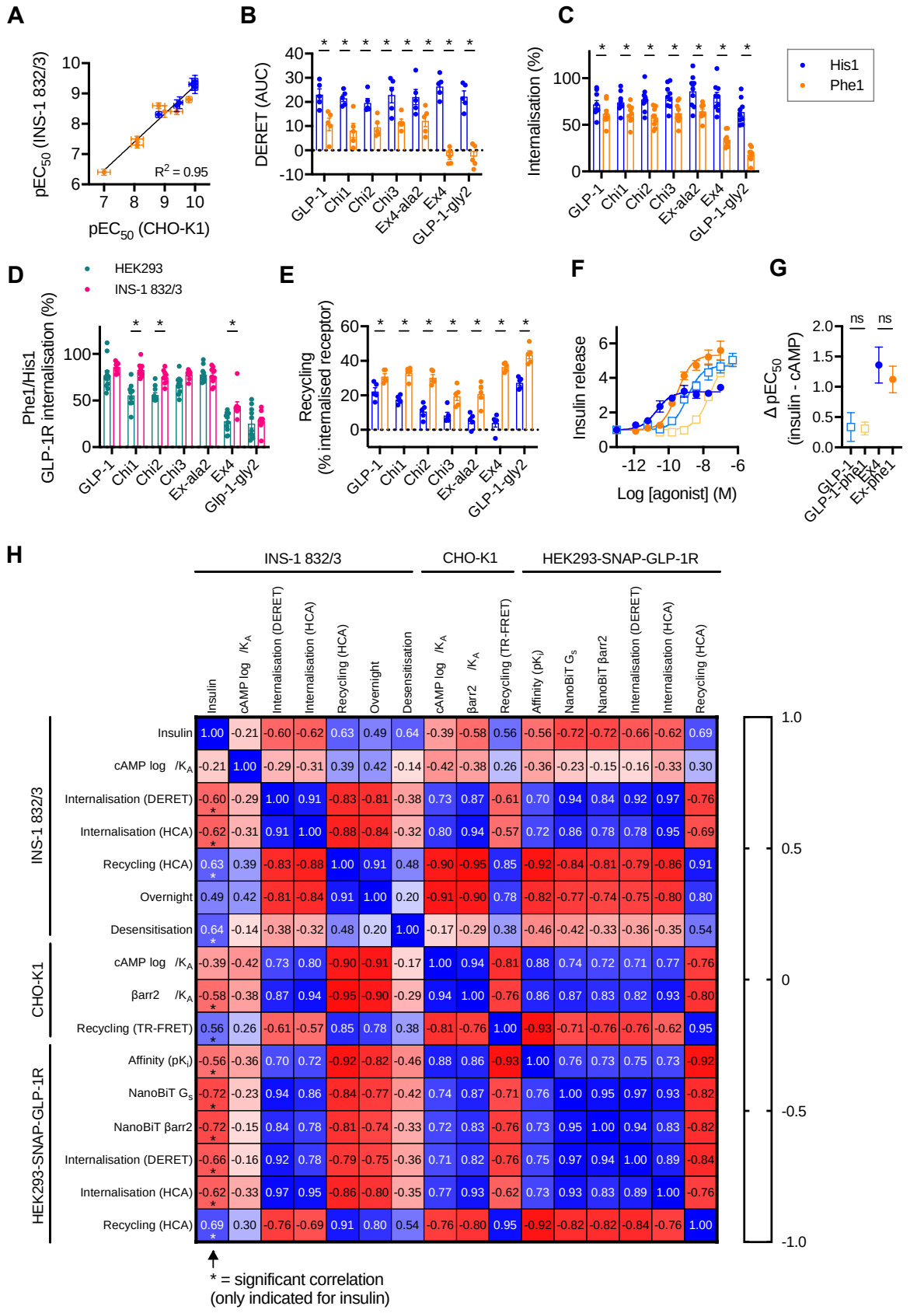
A
B
C
D
E
F
G
H
pEC50 (INS-1 832/3)
pEC50 (CHO-K1)
R2 = 0.95
DERET (AUC)
Internalisation (%)
His1
Phe1
HEK293
INS-1 832/3
Phe1/His1 GLP-1R internalisation (%)
Recycling (% internalised receptor)
Insulin release
Log [agonist] (M)
Δ pEC50 (insulin - cAMP)
ns
GLP-1
Chi1
Chi2
Chi3
Ex-ala2
Ex4
Glp-1-gly2
GLP-1-gly2
GLP-1-phe1
Ex-phe1
INS-1 832/3
CHO-K1
HEK293-SNAP-GLP-1R
Insulin
cAMP log /KA
Internalisation (DERET)
Internalisation (HCA)
Recycling (HCA)
Overnight
Desensitisation
βarr2 /KA
Recycling (TR-FRET)
Affinity (pKi)
NanoBiT Gs
NanoBiT βarr2
* = significant correlation
(only indicated for insulin)

Figure S-3. Effects in beta cells. (**A**) Comparison of acute cAMP potencies in CHO-K1-βarr2-EA-GLP-1R and INS-1 832/3 cells by linear regression. (**B**) Alternative representation of heatmap data from Figure 3B, i.e. DERET-measured GLP-1R internalisation AUC in INS-1 832/3 GLP-1R$^{-/-}$ cells stimulated with 1 µM agonist, *n*=5, statistically compared by one-way randomised block ANOVA with Sidak's test for each His1 *versus* Phe1 ligand pair. (**C**) Quantification of SNAP-GLP-1R internalisation in INS-1 832/3 GLP-1R$^{-/-}$ cells after 1 µM ligand treatment for 30 minutes, measured by high content microscopy analysis, *n*=9, with statistical comparison by one-way randomised block ANOVA with Sidak's test to compare bias for each His1 / Phe1 ligand pair. (**D**) Comparison of Phe1 ligand internalisation measurements in INS-1 832/3 cells in comparison to HEK293 cells (see Figure S-2I), with the response of each Phe1 ligand expressed relative to that of its His1 counterpart for each assay, with statistical comparisons performed by one-way ANOVA with Sidak's test. (**E**) As for (C), but for GLP-1R recycling after 1 µM ligand pre-treatment, *n*=5. (**F**) Insulin secretion from wild-type INS-1 832/3 cells treated with 11 mM glucose ± indicated agonist dose for 16 hours, expressed relative to vehicle, *n*=5. (**G**) Comparison of potency estimates for acute cAMP signalling (Figure 3A, Table 5) and sustained insulin secretion (Figure S-3F) performed by subtraction pEC_{50} values, with error propagation, one-way ANOVA with Sidak's test for each His1 *versus* Phe1 ligand pair. (**H**) Correlation matrix summarising relationship between agonist responses included in this work; single-dose responses are normalised on a 0 – 100% scale, whereas logarithmically quantified indices (pK_i, log τ/K_A) have not been further normalised; Pearson r coefficient is shown for each comparison, with significance indicated by asterisks (only for relationships for insulin secretion). *p<0.05 by statistical test indicated in the text. Data represented as mean ± SEM, with individual replicates shown throughout.